Patterned Arrays of Au Rings for Localized Surface Plasmon Resonance

Sarah Kim,[†,‡] Jin-Mi Jung,[‡] Dae-Geun Choi,[§] Hee-Tae Jung,[‡] and Seung-Man Yang*[,†,‡]

National Creative Research Initiative Center for Integrated Optofluidic Systems, Korea Advanced Institute of Science and Technology, Daejeon 305-701, Korea, Department of Chemical and Biomolecular Engineering, Korea Advanced Institute of Science and Technology, Daejeon 305-701, Korea, and Nano-mechanical Systems Research Center, Korea Institute of Machinery & Materials, 171 Jang-dong, Yuseong-gu, Daejeon 305-343, Korea

Received March 3, 2006. In Final Form: June 26, 2006

In this paper, we examined the characteristic behavior of localized surface plasmon resonances (LSPR) of Au dot and ring arrays in response to the selective binding of biomolecules. To do this, patterned arrays of Au rings and dots with various feature scales were fabricated over large areas by an imprint lithography technique. Our results showed that the LSPR spectra of the Au nanorings exhibited a blue shift with increase in the ring widths and asymptotically converged to those for Au nanodots. This clearly implies that the LSPR spectra can be tuned over an extended wavelength range by varying the ring width. For an illustrative purpose, the patterned Au structures were used to detect the binding of streptavidin to biotin. In doing this, the Au patterns were chemically modified with G4 dendrimers of amine terminated poly(amidoamine), which facilitated the tethering of biotin onto the Au pattern. Exposure of the biotinylated Au nanorings to aqueous streptavidin solution induced both red-shifts of the LSPR spectra and changes in the peak intensities. The sensitivity of the LSPR spectra to the binding of the biomolecules was enhanced as the ring width of Au rings was decreased.

Introduction

Nanopatterned metals such as Au and Ag have attracted great interest because of a wide range of applications in bioanalitical chemistry,[1] bioimaging,[2] and biosensors.[3,4] For example, SPR-based biosensors of patterned noble metals have been used to examine a number of ligand−receptor interactions including antibody−antigen, protein−DNA, and DNA−DNA interactions.[5−7] In particular, LSPR utilizes a collective oscillation of the conduction band electrons that arises in the metal nanopatterns when excited by an electromagnetic radiation at a specific wavelength. Generally, the position of the extinction wavelength λ_{max} and the peak shape are related to the shape, size, and composition of the nanopatterns, as well as the feature distance and the external dielectric environment. The extinction spectra of the metal nanopattern exhibit readily measurable wavelength shifts that correspond to small changes in the refractive index within the electromagnetic fields surrounding the nanopattern.[5]

Recent advances in the metal nanostructures have led to the realization of nanopatterns of shells,[8] rods,[9] cups,[10] rings, and disks.[11,12] These developments have provided with the necessary tools to investigate the plasmon properties of a metal nanopattern with an arbitrary geometry. The electromagnetic interactions as a function of the geometric features of metal nanopatterns have been examined by probing the LSPR of hexagonal, square, and linear arrays of Au and Ag with various shapes, which have been fabricated with electron beam lithography or nanosphere lithography.[11,12] The electron beam lithography provides the resolution and integration density required for the practical application but with the level of throughput rate far below the requirement. Meanwhile, the nanosphere lithography affords the controllability in varying the feature size and shape and can produce the nanorings with controllable diameter and wall thickness.[4,8,11] However, defect control over large areas still limits the practical applications of the nanosphere lithography.

Here, we report a novel method of nanoimprint lithography for fabricating patterned arrays of Au rings and dots. The imprint lithography has been considered as a promising high throughput and reproducible nanopattern technique.[13−15] Specifically, we examined the characteristic behavior of the LSPR spectra of the patterned arrays of Au rings and dots by varying either the Au dot size or the width of Au rings. In addition, we have demonstrated that the patterned Au rings or dots could be used for detecting the selective binding between biotin and streptavidin (SA) through the LSPR spectra. Exposure of the biotinylated Au nanorings to aqueous streptavidin solution induced both red-shifts of the LSPR spectra and changes in the peak intensities. For the Au ring array, the LSPR sensitivity to the surface

* To whom correspondence should be addressed. E-mail: smyang@kaist.ac.kr.

† National Creative Research Initiative Center for Integrated Optofluidic Systems, Korea Advanced Institute of Science and Technology.

‡ Department of Chemical and Biomolecular Engineering, Korea Advanced Institute of Science and Technology.

§ Korea Institute of Machinery & Materials.

(1) Srivastava, S.; Frankamp, B. L.; Rotello, V. M. *Chem. Mater.* **2005**, *17*, 487−490.

(2) Wark, A. W.; Lee, H. J.; Corn, R. M. *Anal. Chem.* **2005**, *77*, 3904−3907.

(3) Kanda, V.; Kariuki, J. K.; Harrison D. J.; McDermott, M. T. *Anal. Chem.* **2004**, *76*, 7257−7262.

(4) Haes, A. J.; Chang, L.; Klein, W. L.; Van Duyne, R. P. *J. Am. Chem. Soc.* **2005**, *127*, 2264−2271.

(5) Endo, T.; Kerman, K.; Nagatani, N.; Takamura, Y.; Tamiya, E. *Anal. Chem.* **2005**, *77*, 6976−6984.

(6) Hutter, E.; Fendler, J. H. *Adv. Mater.* **2004**, *16*, 1685−1706.

(7) Fernandes, R.; Yi, H.; Wu, L.; Rubloff, G. W.; Ghodssi, R.; Bentley, W. E.; Payne, G. F. *Langmuir* **2004**, *20*, 906−913.

(8) Prodan, E.; Radloff, C.; Halas. N. J.; Nordlander, P. *Science* **2003**, *302*, 419−422.

(9) Jana, N. R.; Gearheart, L.; Murphy, C. J. *J. Phys. Chem. B* **2001**, *105*, 4065−4067.

(10) McLellan, J. M.; Geissler, M.; Xia, Y. *J. Am. Chem. Soc.* **2004**, *126*, 10830−10831.

(11) Aizpurua, J.; Hanarp, P.; Sutherland, D. S.; Käll, M.; Bryant, G. W.; Gracía de Abajio, F. J. *Phy. Rev. Lett.* **2003**, *90*, 057401.

(12) Hick, E. M.; Zou, S.; Schatz, G. C.; Spears, K. G.; Van Duyne, R. P. *Nano Lett.* **2005**, *5*, 1065−1070.

(13) Suh, K. Y.; Lee, H. H. *Adv. Funct. Mater.* **2002**, *12*, 405−413.

(14) Chou, S. Y.; Krauss, P. R.; Renstrom, P. J. *Appl. Phys. Lett.* **1995**, *67*, 3114−3116.

(15) Chou, S. Y.; Krauss, P. R.; Tenstrom, P. J. *Science* **1996**, *272*, 85−87.

10.1021/la0605844 CCC: $33.50
Published on Web 07/13/2006

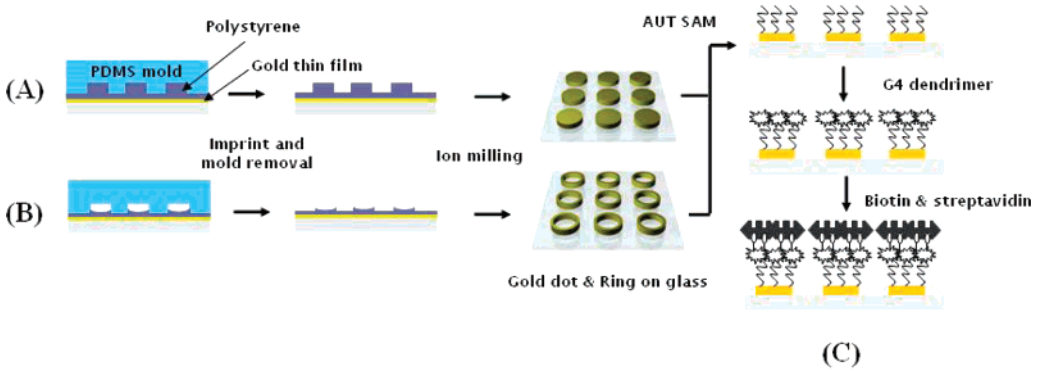

Figure 1. Schematic of nanopatterning of Au islands fabricated by imprint lithography and ion milling. (A and B) Dot and ring pattern formation using thick and thin PS films, respectively. (C) Procedure for immobilizing SA protein on the Au patterns using the SAM of amino-terminated PAMAM dendrimers as an intermediate coupling layer. Sulfo-NHS-LC-biotin was used to bind the SA protein.

modifications was enhanced as the ring width was reduced. In particular, the Au rings with 70 nm thick shells exhibited a change in the LSPR peak position 4−5 times as large as that for the Au dots of the same size, when their surfaces were modified by the binding of SA.

Experimental Section

In Figure 1, the nanoimprint patterning process is schematically illustrated. First, Au layer of 40 nm in thickness was deposited on a glass substrate using an e-beam evaporator. A thin (2 nm) chromium under-layer was pre-deposited to enhance adhesion of the Au layer to the substrate. Then, polystyrene (PS) solutions at various concentrations (1.5, 0.8, and 0.5 wt %, M_w of PS: 45 730) were spin-coated onto the thin Au films. The polymeric film was annealed at a temperature above the glass transition temperature T_g and imprinted with a pre-designed composite PDMS mold, which was fabricated by following a standard procedure. This imprint process took 30 min to 1 h under a low pressure of 1.60 kPa in a vacuum at 150 °C. In scheme A of Figure 1 for high PS concentrations, the PS film was thick enough to fill the cylindrical holes between the PDMS mold and the substrate. Meanwhile, at low PS concentrations below 0.8 wt %, the PS film was thin and partially filled the gap as illustrated in scheme B of Figure 1. In this case, the PS film climbed the PDMS walls under the action of capillary forces and formed the circular undulations around the walls. The PS patterns were treated with reactive ion etching (RIE) of CF_4/O_2 to remove the residual PS layers on the substrate. The RIE modified slightly the feature sizes of the PS patterns. After being cooled to room temperature, the PS patterns were used as mask for Ar ion milling for 2 min, which left behind the patterned Au arrays. The DC bias for the ion milling was 400 V, and the Ar pressure was kept below 5×10^{-4} Torr. In particular, the thin circular PS dots with undulated edges produced eventually the patterned Au rings as shown in scheme B of Figure 1. Finally, the residual PS mask was removed by sonicating the substrate in toluene for 15 min.

To modify the surfaces of Au islands, we used self-assembled monolayer (SAM) of aminoundecanethiol (AUT) as shown in scheme C of Figure 1. To ensure a well organized SAM of AUT onto the Au islands, the sample was incubated in the AUT solution for 24 h. After careful rinsing and thorough drying with pure N_2 gas, the patterned Au array was activated by incubating in 10 mM of bis-[sulfosuccinimidyl] suberate (BS^3) in phosphate buffered saline (PBS) solution. Subsequently, the substrate was incubated overnight in 10 wt % methanolic solution of G4 dendrimers of amine terminated poly(amidoamine) (henceforth, PAMAM). Then, the anchored PAMAM was biotinylated by attaching sulfo-NHS-LC-biotin covalently via amid bond formation. Finally, the biotinylated Au dot and ring arrays were exposed to 20 μM streptavidin solution to induce the binding of streptavidin to the biotinylated Au surface. LSPR was measured on UV−visible near-IR spectroscopy (JASCO: V-570) of the double-beam system with a monochromator. The scanning wavelength ranged from 300 to 2500 nm. The light source was an unpolarized halogen lamp (200∼2500 nm). AFM (Seiko Instruments: SPA 400) was used to obtain topographic images of the nanopattern arrays. The images were taken with contact mode under ambient conditions.

Results and Discussion

LSPR of Bare Au Dot and Ring Patterns. We prepared Au arrays of four different features, namely, Au dots DA and DB of 400 and 800 nm in diameter, respectively and Au rings RA1, RA2, and RA3 of 150, 120, and 70 nm in ring width, respectively. All rings were 400 ± 20 nm in outer diameter. The Au dot patterns DA and DB were obtained using relatively thick PS films which were spin-cast with 1.5 wt % PS solution. Meanwhile, the ring patterns RA1 and RA2 were produced with 0.8 wt % PS solution and RA3 was produced with 0.5 wt % PS solutions using the same PDMS stamp as that for Au dots (DA) of 400 nm in diameter. Prolonged RIE with CF_4/O_2 for 10 s longer reduced the ring width from 150 nm (RA1) to 120 nm (RA2). Large area SEM images of Au dots (DA) and rings (RA2) are shown in Figure 2 with the corresponding AFM images in the insets. The whole area of each pattern was 5 mm × 5 mm. The island densities of Au dots and rings were approximately 10^8 dots/cm^2. Considering that the probing area of the LSPR extinction was approximately 0.2 cm^2, the optical data were collected and averaged over $\approx 2 \times 10^7$ dots or rings.

Figure 3 shows the LSPR spectra of five different "bare" Au patterns; namely, arrays of Au dots DA and DB and Au rings RA1, RA2, and RA3. As noted in Figure 3, the LSPR spectra were modulated by the feature size and shape of dots and rings. For example, the extinction wavelength was blue shifted from $\lambda_{max} = 2290$ to 1440 nm as the dot size was reduced from 800 to 400 nm in diameter. Meanwhile, the LSPR peaks of RA1, RA2, and RA3 appeared at 1600, 1890, and 2180 nm, respectively. This clearly indicated that, when the central part of a Au dot was removed forming a Au ring, the extinction wavelength is shifted toward near-infrared region and the degree of red-shift and the peak broadening were very sensitive to the ring widths. This tendency was consistent with the previous result for dots and rings which were prepared by nanosphere lithography.[11]

The difference in the LSPR spectra of Au dots and rings can be understood by analyzing the particular modes that are most efficiently excited for each type of pattern. In the ring, there is a strong electromagnetic coupling between the inner and outer walls of the Au ring when the ring width is small compared to the ring radius. Therefore, the LSPR peak position could be tuned by changing the dot size and the width of the Au ring in the near-IR range (1400−2200 nm) of wavelength. This tunability is similar to the case of red-shift which occurs when the thickness

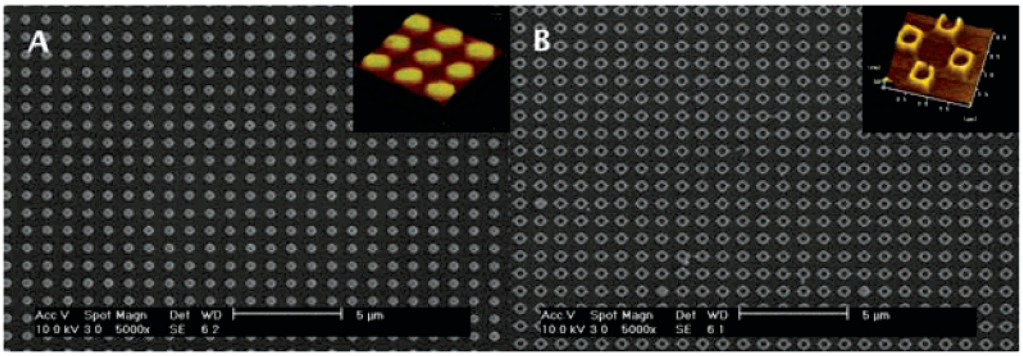

Figure 2. SEM and AFM images of Au dot and ring nanopatterns. A. Au dots DA of 400 nm in diameter created using 150 nm thick PS film cast with 1.5 wt % PS solution. B. Au rings RA2 of 400 nm in outer diameter with 120 nm ring width created using 100 nm thick PS film cast with 0.8 wt % PS solution.

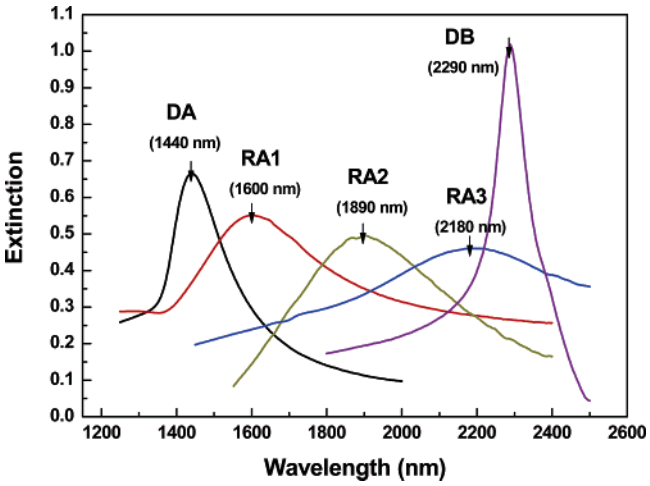

Figure 3. LSPR spectra of Au nanopatterns for various dot sizes and ring widths. DA: 400 nm dots, DB: 800 nm dots, RA1: 400 nm rings of 150 nm width, RA2: 400 nm rings of 120 nm width, RA3: 400 nm rings of 70 nm width. DA, RA1, RA2, and RA3 were obtained from the identical master stamp by changing the PS film thickness and RIE time. The height of all Au islands was 40 nm.

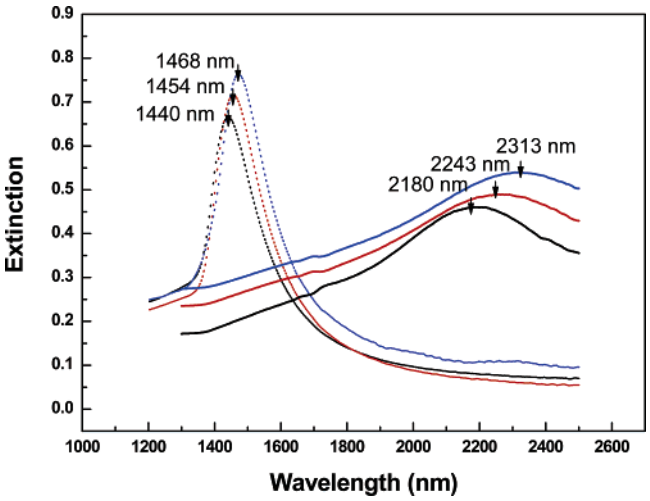

Figure 4. Characteristic behavior of the LSPR spectra in response of the surface modifications of Au dots (DA) and Au rings (RA3). Dashed lines are for Au dots and solid lines for Au rings. Black lines: LSPR spectra of "bare" Au dots and rings. Red lines: LSPR spectra of G4 tethered Au dots and rings. Blue lines: LSPR spectra of G4 and SA anchored Au dots and rings.

of metallic spherical nanoshells is decreased. In this case, Mie scattering theory explained that the nanoshell plasmon shifts to lower energy with decrease in the shell thickness are due to an increased interaction between the sphere and cavity plasmons, resulting in increased splitting between two hybrid plasmons.[8]

Thus far, we showed that the LSPR of "bare" Au nanodot and ring patterns formed by imprint lithography can be implemented using extremely simple, low cost equipment for visible and near-IR extinction spectroscopy. Furthermore, the feature spacing and the positions of dot or ring islands can be controlled readily since they are immobilized on the substrate. Here, for an illustrative purpose, we conducted a biological sensing test using our patterned arrays of Au rings and dots. To do this, streptavidin (SA) was chosen as a target molecule, which is one of the most prevalent and important proteins used in affinity-based diagnostics and separations.[16]

LSPR of the Surface-Modified Au Dot and Ring Patterns. In this study, the LSPR spectra and λ_{max} of Au nanodots and rings were monitored during the surface modification step. The anchored PAMAM played a role of linker molecules and endowed additional sensitivity of LSPR to the binding of SA. The greater protein immobilization efficiency of nanodot or ring pattern arises from the particular three-dimensional steric arrangement of the large number of amine groups available for covalent coupling that is present on the PAMAM surface.[17] In Figure 4, we examined the sensitivity of the plasmon response of the 400 nm Au dot (DA) or 400 nm Au ring (RA3) pattern to the binding of SA protein with sulfo-NHS-LC-biotin. The changes in the LSPR spectra were displayed as the Au dots and rings were modified by the sequential anchoring of PAMAM and SA. Specifically, the anchoring of PAMAM to the 400 nm Au dot (DA) array induced a red-shift of the LSPR spectra by 14 nm as shown in Figure 4. Then, the subsequent binding of SA resulted in a further red-shift of the LSPR peak by again 14 nm. Also noted from Figure 4 is that the peak intensity was increased by the anchoring of PAMAM and SA. Similarly, for the Au ring (RA3) array, the LSPR spectra were modified also in response to the attachment of biomolecules. However, the LSPR peak positions of 400 nm Au rings (RA3) were much more sensitive to the surface modification than those of 400 nm Au dots (DA). Figure 5 summarizes the LSPR peak shifts in response to the surface modifications of five different Au islands considered here. As noted, the LSPR spectra for 800 nm Au dot array DB show that the LSPR peak position was not modulated so clearly as those for 400 nm dot array DA by the surface modifications. For Au ring patterns, the LSPR peak shift in response to the successive

(16) Mark, S. S.; Sandhyarani, N.; Zhu, C.; Campagnolo, C.; Batt, C. A. *Langmuir* **2004**, *20*, 6808−6817.

(17) Benters, R.; Niemeyer, C. M.; Drutschmann, D.; Blohm, D.; Wöhrle, D. *Nucleic Acids Res.* **2002**, *30*, e10.

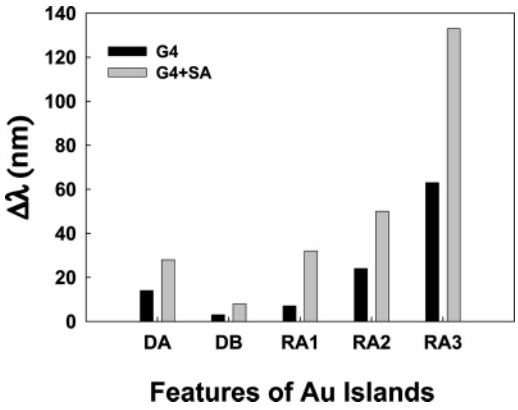

Figure 5. Bar chart of the changes in the LSPR peak shifts ($\Delta\lambda$) relative to those for bare Au patterns with successive anchoring of G4 and SA onto five different Au patterns, DA, DB, RA1, RA2, and RA3. Black bars are for G4 anchored Au patterns and gray bars for G4 and SA anchored Au patterns.

attachments of PAMAM and SA was strongly dependent on the ring width. It can be seen from Figure 5 that, as the width of the Au ring became thinner, the sensitivity based on the peak shift was improved for detecting the attachments of PAMAM and SA. According to Mie scattering theory, any variation in the refractive index of the surface layer should lead to changes in the intensity and position of the SPR peak.[14] In this case, the biomolecules attached to the Au ring would increase the effective average refractive index of the surface layer of the Au nanoring and thus caused the red shift of the SPR peak. In general, the LSPR sensitivity is closely related to changes in the refractive index of the environment and the effective volume of the Au patterns which are modified with attached molecules.[19,20] For the Au ring array, the LSPR sensitivity is enhanced more due to the increase in the effective refractive index and the decrease in the relative volume by the surface modification than that for the dot array. Consequently, the change in the refractive index due to the binding of PAMAM or SA becomes more significant as the ring width is deceased. In particular, the Au rings with 70 nm width exhibited a change in the LSPR peak shift 4.5 times larger than that for the Au dots of the same size, when their surfaces were modified by the binding of SA. Although the contact area between Au and biomolecules in the ring structure is much smaller than that in the dot structure, the peak shift caused by the adsorption was larger as shown in Figure 5. Recently, Sun et al. reported similar experimental results that a hollow sphere was more sensitive to local dielectric changes than a solid sphere of the same size. They found that, for particles with a diameter of 50 nm, the SPR sensitivity of the nanoshells with a shell thickness of 4.5 nm was almost 600% greater than that of solid Au nanospheres.[21]

In conclusion, Au dot and ring patterns were fabricated by imprint lithography under the action of capillary forces. These patterned structures were successfully used for probing the binding of biomolecules to demonstrate the potential applications of the Au island arrays as the LSPR-based biosensors. The ring width could be tuned simply by varying the concentration of the PS solution which was used as the polymeric mask. As a result, the characteristic behavior of the LSPR spectra could be readily controlled. Finally, we examined the LSPR sensitivity of the Au dot and ring patterns to the binding of biotin and SA using PAMAM dendrimers as linkers. Small dots were found to be more sensitive in detecting the biomaterials than large ones. In addition, thinner ring structure also led to further signal enhancement in response to the surface modifications. Understanding the parameters that control the sensitivity will offer insight toward the design and engineering of biosensors based on LSPR responses.

Acknowledgment. This work was supported by a grant from the Creative Research Initiative Program of the Ministry of Science & Technology for "Complementary Hybridization of Optical and Fluidic Devices for Integrated Optofluidic Systems". The authors also acknowledge partial support (M102KN010002-04K1401-00212) from the Center for Nanoscale Mechatronics and the Brain Korea 21 Program.

LA0605844

(18) Bohren, C. F.; Huffman, D. R. *Absorption and Scattering of Light by Small Particles*; Wiley: New York, 1983.
(19) Prodan, E.; Lee, A.; Nordlander, P. *Chem. Phys. Lett.* **2002**, *360*, 325−332.
(20) Alvarez, M. M.; Khoury, J. T.; Schaaff, T. G.; Shafigullin, M. N.; Vezmar, I.; Whetten, R. L. *J. Phys. Chem. B* **1997**, *101*, 3706−3712.
(21) Sun, Y. G.; Xia, Y. N. *Anal. Chem.* **2002**, *74*, 5297−5305.
(22) Odom, T. W.; Love, J. C.; Wolfe, D. B.; Paul, K. E.; Whitesides, G. M. *Langmuir* **2002**, *18*, 5314−5320.